RESEARCH

Beauty in motion through the lens of doppler's formula

Ramzi Suleiman

Suleiman R. Beauty in motion through the lens of doppler's formula. J Pure Appl Math. 2023; 7(5):297-305.

ABSTRACT

Despite ample research on beauty in nature and in mathematical representations of natural phenomena, we are unaware of studies in physics and mathematics devoted to the objective beauty induced by motion, regardless of the aesthetic qualities of the moving body. We undertake this objective by focusing on the Doppler formula, which describes the shifts in wave frequencies caused by the motion of the wave's source relative to a human observer or receiver. We uncover several fascinating golden ratio, and silver ratio symmetries, in the base formula and its mathematical moments. Furthermore, we allude to existing applications of the Doppler Effect in conjunction with the golden ratio in computer-generated music, and sonar image-detection technology. We also propose a similar usage of golden ratio symmetries in the rapidly developing applications of Wi-Fi and smartphones to sense human motion. In addition, we point to appearances of the Doppler formula and its moments in quantum physics, and the relativity of information, and conclude by contemplating the possibility of a deeper level of physical reality.

Key Words: *Doppler effect; Doppler formula; Mathematical beauty; Beauty in motion; Golden ratio; Silver ratio; Metallic ratios; Continued fractions; Penrose tiles; Electronic music; Sonar imaging; Doppler radar.*

INTRODUCTION

Leading mathematicians, physicists, philosophers, and other scholars have underscored the importance of mathematical beauty. Isaac Newton, Paul Dirac, Hermann Weyl, and Bertrand Russell, for example, glorified the experience derived from such beauty, comparing it with appreciating the greatest works of art [1-4]. Semir Zeki, a founding father of neuroesthetics, demonstrated in an fMRI study that, when mathematicians' brains see an equation they consider beautiful, it activates the same part of the brain as when they perceive a painting or music as beautiful [5, 6].

Paul Dirac, an advocate of the importance of mathematical beauty in physics, believed that the beauty of a mathematical equation might be an indication that it describes a fundamental law of nature. In describing his method in theoretical physics, he wrote: "A good deal of my research work in physics has consisted in not setting out to solve some particular problem but simply examining mathematical quantities of a kind that physicists use and trying to fit them together in an interesting way regardless of any application that the work may have. It is simply a search for pretty mathematics. It may turn out later that the work does have an application. Then one has had good luck" [7]. Dirac believed that it is a feature of nature that "fundamental physical laws are described in terms of great beauty and power" [1]. A similar opinion was also expressed by Zelinger, who argued that the "mathematical beauty of the theory is a strong argument for its robustness." Zelinger further argued that "we might expect that physical and mathematical structures would share the characteristics that we call beauty, and from an evolutionary perspective, the human sense of beauty could have evolved to find natural patterns pleasing" [8].

Beauty in motion

The bulk of research on beauty in motion comes from dance, film and video, and kinetic art [9-14]. Although numerous scientific papers and books have been written on beauty in nature and in mathematical representations of natural phenomena, this author is not aware of any study in physics, mathematics, or other science devoted to beauty in motion itself [15-20]. This neglect is unjustified, given the fact that everything in the universe, at all scales, is in continuous motion. In cosmology and astrophysics, all observed structures are in continuous motion relative to us; further, information about cosmological objects and phenomena is deduced from light and other types of emitted waves. At the nanoscale, most information on small particle physics and quantum phenomena is deduced by information-carrying waves. The same applies to all phenomena at all scales.

Professor Emeritus, CEO, Accura-c LTD, University of Haifa, Israel

Correspondence: Ramzi Suleiman, Professor Emeritus, CEO, Accura-c LTD, University of Haifa, Israel, E-mail: suleiman@psy.haifa.ac.il
Received: Aug 1, 2023, Manuscript No. puljpam-23-6629, Editor Assigned: Aug 2, 2023, Pre-QC No. puljpam-23-6629 (PQ), Reviewed: Aug 20, 2023, QC No. puljpam-23-6629 (Q), Revised: Sep 15, 2023, Manuscript No. puljpam-23-6629 (R), Published: Sep 30, 2023, DOI:-10.37532/2752-8081.23.7(5).297-305

Here, we focus on the following question: Is there an intrinsic beauty in motion? Since the bulk of information about the motion of objects, relative to observers and their measurement devices, are carried by sound or light waves, we inquire about the aesthetics of motion as mirrored by the Doppler formula. Our analysis hereafter is theoretical, but all its results are experimentally testable.

The rest of this paper is organized as follows: In Section 3, we give a brief reminder of the Doppler effect and its formula. In Section 4, we uncover hidden harmonious beauties of the Doppler formula, with special attention given to symmetry properties and the appearances of golden and silver ratios in the Doppler formula and its mathematical moments. In Section 5, we uncover another source of beauty by showing that Fourier transforms of the base formula and its moments are simple sinusoids and remark briefly on practical application of the results in the design of linear systems. In Section 6, we present two existing applications of the aesthetics embedded in the Doppler effect, i.e., in computer-generated music and in sonar image-detection technology. We also propose similar usage in the rapidly developing applications of the Doppler shift in Wi–Fi and smartphones for sensing human motion. In Section 7, we allude briefly to other manifestations of the Doppler formula and its moments in other fields of physics. In Section 8, we conclude and contemplate the possibility of a deeper level of reality, at which the various fields in which the same equation appears are connected.

Doppler Formula

The Doppler effect is the phenomenon by which the frequency of a wave emitted from a source appears to be increased when the source and observer approach one another and decreased when they are receding from one another (as compared with the frequency of the same source when it is at rest with respect to the observer) [21, 22].

Herbert Dingle argued, "It is doubtful if there is a serious rival to the Doppler effect, as the department of modern science in which the experimental basis is slightest in comparison with the structure raised on it [23]. Most of our knowledge of stellar motions, including the characteristics of binary stars, the evidence for the rotation of the galaxies, and the whole phenomenon known as 'the expansion of the universe' consists of deductions from this one principle. It would be fair to say that, without it, cosmology would scarcely exist as a scientific subject" [23]. Since the above-cited paragraph was published in 1860, the volume of present research on the Doppler effect light, sound, seismic waves, and other forms of wave motion and its technological applications have soured up exponentially. Measurement of the Doppler redshift is now pivotal to cosmology and astrophysics. Redshift probes are essential in cosmological surveys, in measuring the rate of expansion of the accelerating universe, the structure and rotational velocities of galaxies and galaxy clusters [24-28]. In technology, the Doppler shift is used in medical ultrasonography, radars, sonars, Acoustic Doppler Current Profilers (ADCPs), and more [29-37].

For a receding source from an observer, the Doppler effect is captured by the Doppler formula

$$f_r = f_s \frac{c-v}{c+v}, \tag{1}$$

where f_r is the measured frequency at the receiver, f_s is the measured frequency at the source, c is the velocity of the signal relative to the medium between the source and the receiver, and v is the velocity of the source relative to the receiver. For an approaching source, the negative and positive signs should be interchangeable.

Equation (1) could be rewritten as

$$\frac{f_r}{f_s} = \frac{1-\beta}{1+\beta}, \tag{2}$$

where $\beta = \frac{v}{c}$.

Hidden beauty in the Doppler Formula

The function in the right side of Eq. (2) has an apparent beauty. Interchanging the negative and positive signs in the nominator and denominator results in the inverse function $\frac{1}{(\frac{f_r}{f_s})}$. This apparent symmetry is the surfacing tip of more surprising beautiful symmetries.

First, denote the ratio $\frac{f_r}{f_s}$ by $F(\beta)$, and allow β to exceed unity, then for number α the function $F(\beta)$ satisfies

$$F(\beta^\alpha) = -F(\beta^{-\alpha}). \tag{3}$$

Proof:

$$-F(\beta^{-\alpha}) = -\frac{1-\beta^{-\alpha}}{1+\beta^{-\alpha}} = -\frac{\beta^\alpha-1}{\beta^\alpha+1} = \frac{1-\beta^\alpha}{1+\beta^\alpha} = F(\beta^\alpha). \tag{4}$$

As examples, for $\alpha = 1$:

$$F(\tfrac{1}{2}) = \frac{1-\frac{1}{2}}{1+\frac{1}{2}} = \frac{1-\frac{1}{2}}{1+\frac{1}{2}} = \frac{1}{3} = -\frac{1-2}{1+2} = -F(2), \tag{5}$$

$$F(\tfrac{1}{\sqrt{2}}) = \frac{1-\frac{1}{\sqrt{2}}}{1+\frac{1}{\sqrt{2}}} = \frac{\sqrt{2}-1}{\sqrt{2}+1} = -\frac{1-\sqrt{2}}{1+\sqrt{2}} = -F(\sqrt{2}). \tag{6}$$

Second, it is easy to show that for any two real values a, and b of β:

If $F(a) = b$, then $F(b) = a$ (7)

Examples, $F(0) = 1$, and $F(1) = 0$; $F(\frac{1}{3}) = \frac{1}{2}$, and $F(\frac{1}{2}) = \frac{1}{3}$; $F(\frac{2}{3}) = \frac{2}{10}$, $F(\frac{2}{10}) = \frac{2}{3}$; and for a randomly picked number 0.214632, we have $F(0.2146320) \approx 0.646589255$, and $F(0.646589255) \approx 0.2146320$.

Third, define $\mathfrak{F}_n(\beta) \triangleq F(F(F(F(\ldots F(\beta)))))$, where n is the number of embeddedness; then, it could be easily shown by induction that

$$\mathfrak{F}_n(\beta) = \begin{cases} \beta, & \text{for } n = 2m \\ \frac{1-\beta}{1+\beta}, & \text{for } n = 2m+1 \end{cases} \tag{8}$$

m = 0, 1, 2, 3,...

Fourth, more surprising symmetries pop up when we look at the *moments* of the function $F(\beta)$, defined as

$$F_n(\beta) = \beta^n F(\beta) = \beta^n \frac{1-\beta}{1+\beta}, \qquad \beta \le 1,\ n \text{ integer n},\ n \ge 1. \tag{9}$$

Figure (1) depicts the moments $F_n(\beta)$ for selected n values ($n \ge 1$). As the figure shows, for all $n \ge 1$, the functions $\{F_n(\beta)\}$ are positively skewed with unique maxima acheived at points β^*_n. Also, as n increases, the points of maxima shift right-wise, with corresponding decrease in the maxima, such that for $n \to \infty$, $\beta^*_\infty \to 1$, $F_n(\beta^*) \to 0$.

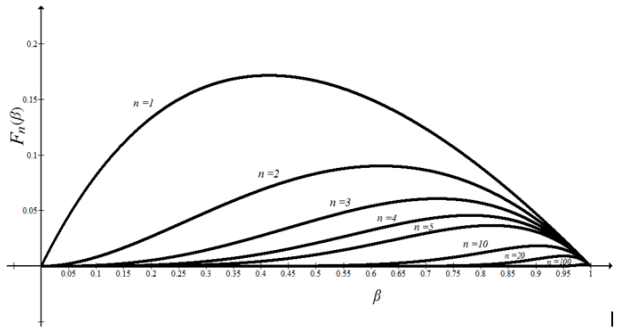

Figure 1) $F_n(\beta)$ *for selected integers* ($n \ge 1$)

To calculate the points of maxima and their corresponding maximum values, we derive $F_n(\beta)$ with respect to β and equate the derivative to zero, yielding

$$n\beta^2 + 2\beta - n = 0, \tag{10}$$

which solves for

$$\beta^*_n = \frac{\sqrt{n^2+1}-1}{n}. \tag{11}$$

With corresponding maxima points equaling

$$F_n(\beta^*_n) = \left(\frac{\sqrt{n^2+1}-1}{n}\right)^n \left(\frac{1-\frac{\sqrt{n^2+1}-1}{n}}{1+\frac{\sqrt{n^2+1}-1}{n}}\right) = \left(\frac{\sqrt{n^2+1}-1}{n}\right)^n \left(\sqrt{n^2+1}-n\right)$$
$$= \frac{1}{n^n}\left(\sqrt{n^2+1}-1\right)^n \left(\sqrt{n^2+1}-n\right) = (\beta^*_n)^n \left(\sqrt{n^2+1}-n\right). \tag{12}$$

Equations (11) and (12) reveal beautiful symmetries. For $n = 1$ $\beta^*_1 = \sqrt{2}-1 = \delta_s (\approx 0.414213562373095)$, where δ_s is the silver ratio [38, 39].

The corresponding maximum is equal to

$$F_1(\beta^*_1) = (\sqrt{2}-1)^2 \approx \delta_s^2 \qquad (\approx 0.1715728752538099). \tag{13}$$

For $n = 2$, Eq. (11) yields

$$\beta^*_2 = \frac{\sqrt{2^2+1}-1}{2} = \frac{\sqrt{5}-1}{2} = \varphi \approx 0.618033988749895, \tag{14}$$

where φ is the famous golden ratio [40-41]. The golden and silver ratios are two famous irrational numbers. Their simple continued fractions are, respectively,

$$\varphi = \frac{\sqrt{5}-1}{2} = \frac{1}{1+\frac{1}{1+\frac{1}{1+\cdots}}} \tag{15}$$

$$\delta_s = \sqrt{2}-1 = \frac{1}{2+\frac{1}{2+\frac{1}{2+\cdots}}} \tag{16}$$

The golden ratio is intimately related to the Fibonacci sequence of numbers 1, 2, 3, 5, 8, 13, 21, 34, 55, 89, 144, … , defined by the linear recurrence equation

$$f_{n+1} = f_n + f_{n-1}. \tag{17}$$

The golden ratio is the limit of the ratio $\frac{f_{n-1}}{f_n}$ when $n \to \infty$, or

$$\varphi = \lim_{n\to\infty} \frac{f_{n-1}}{f_n} = \frac{\sqrt{5}-1}{2} \tag{18}$$

We prefer to use the symbol δ_s for the ratio $\sqrt{2}-1$ instead of the common use of this notation for its conjugate $\sqrt{2}+1$.

More fascinating mathematical properties of the two ratios and other metallic ratios are detailed in many sources [42-43].

Interestingly, the corresponding maximum of the second moment $F_2(\beta)$ is equal to φ^5. To demonstrate, we substitute $\beta = \varphi$ in Eq. (9):

$$F_2(\varphi) = \varphi^2 \frac{1-\varphi}{1+\varphi}. \tag{19}$$

Using the property $\frac{1}{1+\varphi} = \varphi$, we can write $1 - \varphi = \varphi^2$. Substitutions in Eq. (19) give

$$F_2(\varphi) = \varphi^5 = 0.09016994. \tag{20}$$

Other notable nice properties of the Doppler equation, corresponding to the golden and silver ratios, are

$$F(\sqrt{2}-1) = \frac{1-(\sqrt{2}-1)}{1+(\sqrt{2}-1)} = \frac{2-\sqrt{2}}{(\sqrt{2})} = \sqrt{2}-1 \tag{21}$$

$$F(\varphi) = \frac{1-\varphi}{1+\varphi} = \frac{(1-\frac{1}{1+\varphi})}{1+\varphi} = \frac{\varphi}{(1+\varphi)^2} = \varphi^3 \approx 0.236068\ldots \tag{22}$$

$$F(\varphi^3) = \frac{1-\varphi^3}{1+\varphi^3} = \frac{1-\frac{1-\varphi}{1+\varphi}}{1+\frac{1-\varphi}{1+\varphi}} = \frac{2\varphi}{2} = \varphi \approx 0.618033\ldots \tag{23}$$

The areas under the functions $F_n(\beta)$ ($n \ge 0$) are given by

$$A_n = \int_0^1 F_n(\beta)\, d\beta = \int_0^1 \beta^n \frac{1-\beta}{1+\beta} d\beta. \tag{24}$$

For $n = 0, 1, 2, 3$, we get, respectively, $2\ln(2) - 1$ (≈ 0.386294), $\frac{3}{2} - 2\ln(2)$ (≈ 0.113706), $2\ln(2) - \frac{4}{3}$ (≈ 0.052961), and $\frac{17}{12} - 2\ln(2)$ (≈ 0.030372). Table 1 depicts exact values and eight-digit decimal approximations for the points of maxima β^*_n, the corresponding maxima of $F_n(\beta)$, and the integral $\int_0^1 F_n(\beta)\, d\beta$ for integer n values in the range $0 \le n \le 8$. Note that all the maxima points and the corresponding maxima values are irrational numbers, with the first and second (for n=1, 2) equaling the silver and golden ratio, respectively. The emergence of the golden and silver ratios in the above analysis is quite striking given the fact that this ratio plays a key role in aesthetics,

including in architecture and design, music, quantum physics, neutrino mixing physics, astronomy crystallography, the structure of plants, functioning of the human brain, the social sciences, and much more (Table 1) [44-69].

TABLE 1

Points of maxima x^*_n , maxima, $G(x^*_n)$, and the integral $\int_0^1 G_n(\beta)\, d\beta$ for 1 ≤n ≤8

	Point of maximum β^*_n		*Maximal value* $F_n(\beta^*_n)$		Area $A_n = \int_0^1 F_n(\beta)\, d\beta$	
n	Exact value	Approximation	Exact value	Approximation	Exact value	Approximation
0	0	0	1	1	2 ln(2) -1	0.386294
1	$\sqrt{2}-1=\delta_s$	0.414214	$(\sqrt{2}-1)^2=\delta_s^2$	0.171573	$\frac{3}{2}-2\ln(2)$	0.113706
2	φ	0.618034	φ^5	0.090170	$2\ln(2)-\frac{4}{3}$	0.052961
3	$\frac{1}{3}(\sqrt{10}-1)$	0.720759	$\frac{1}{27}(\sqrt{10}-1)^3(\sqrt{10}-3)$	0.060762	$\frac{17}{12}$ -2ln(2)	0.030372
4	$\frac{1}{4}(\sqrt{17}-1)$	0.780776	$\frac{1}{256}(\sqrt{17}-1)^4(\sqrt{17}-4)$	0.045749	$2\ln(2)-\frac{41}{30}$	0.019628
5	$\frac{1}{5}(\sqrt{26}-1)$	0.819804	$\frac{1}{3125}(\sqrt{26}-1)^5(\sqrt{26}-5)$	0.036667	$-2\ln(2)+\frac{7}{5}$	0.013706
6	$\frac{1}{6}(\sqrt{37}-1)$	0.847127	$\frac{1}{46656}(\sqrt{37}-1)^6(\sqrt{37}-6)$	0.030586	$2\ln(2)-\frac{289}{210}$	0.010104
7	$\frac{1}{7}(\sqrt{50}-1)$	0.867295	$\frac{1}{823543}(\sqrt{50}-1)^7(\sqrt{50}-7)$	0.026233	$-2\ln(2)+\frac{1171}{840}$	0.006136
8	$\frac{1}{8}(\sqrt{65}-1)$	0.882783	$\frac{1}{16777216}(\sqrt{65}-1)^8(\sqrt{65}-8)$	0.022963	$2\ln(2)-\frac{1739}{1260}$	0.006136

As examples in quantum physics, Hardy's nonlocality test shows a maximum nonlocality (in terms of a joint probability) of $(-11 + 5\sqrt{5})/2 = 5\,\varphi - 3 = \varphi^5 \approx 0.09017$, over all possible states of two spin-$\frac{1}{2}$ particles, for all possible choices of observables [49]. More recently, Coldea et al. Demonstrated that applying a magnetic field at right angles to an aligned Ising chain of cobalt niobate atoms makes the cobalt enter a quantum critical state in which the ratio between the first two resonances equals the golden ratio [50]. In plants from vastly different origins, the golden ratio plays a key role in the arrangements of leaves, seeds, and spirals [62]. In a recent study on locomotion, it was reported that the Golden ratio plays a pivotal role in giving harmony to locomotion [70]. In the social sciences, Suleiman showed that in ultimatum games, and in sequential bargaining games, agreements are reached when proposers offer a Golden Ratio division of the goods [68, 69]. The Golden Ratio fairness division of goods suggests that human's sense for fairness, and of visual and auditory beauty, are strongly correlated.

The silver ratio also has many manifestations in aesthetics and science, including in architecture, quantum mechanics, crystallography, and more [71-76]. The beauty of the golden and silver ratio is manifest, respectively, in Penrose fivefold golden ratio tiles, and the Ammann–Beenker aperiodic tiles [77-80]. Two examples of tiles for each symmetry are depicted in Figures 2 and 3.

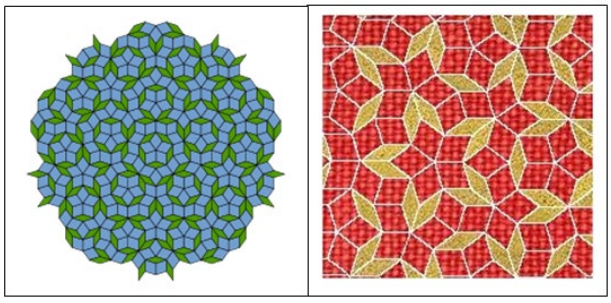

Figure 2) *Two Penrose tiles with fivefold golden ratio symmetries*

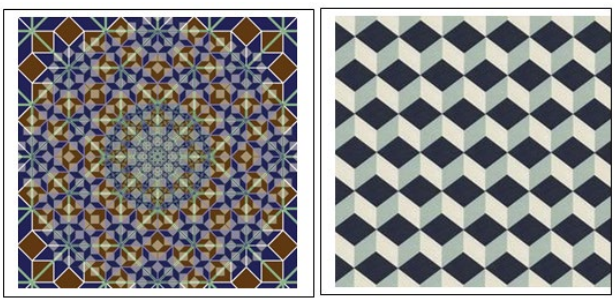

Figure 3) *Two silver ratio patterns*

The Fourier transform of $F_n(\beta)$

The Fourier transform of a function $f(x)$ is defined as

$$\mathbf{F}(\omega) = \int_{-\infty}^{\infty} f(x) e^{-i\omega x}\, dx \ . \qquad (25)$$

Calculation of the Fourier transform of $F_n(\beta)$ $(n \geq 0)$ yields

$$\mathcal{F}\{F_n(\beta)\} = \mathcal{F}\{\beta^n \tfrac{1-\beta}{1+\beta}\} = (-1)^n i \sqrt{2\pi}\, e^{-i\omega}$$

$$= (-1)^n \sqrt{2\pi}\, [\cos(\omega) - i \sin(\omega)] \ . \qquad (26)$$

Thus, the Fourier transforms of the Doppler formula, and all its moments $F_n(\beta)$, $(n \geq 1)$, turn out to be simple sinusoids.

This result hints at possible applications of the Doppler family of moments in mathematics and engineering, particularly in linear dynamical systems, in which the output $y(t)$ is the mathematical convolution between the input function, $x(t)$ and the system response function $h(t)$ defined or

$$y(t) = \int_{-\infty}^{\infty} x(t-\tau)\,)\, h(\tau)\, d\tau \ . \qquad (27)$$

For such systems, the Fourier transform of the output $Y(\omega)$ is the algebraic product of the Fourier transforms of $x(t)$ and $h(t)$:

$$Y(\omega) = X(\omega)\ .\ H(\omega) \qquad (28)$$

Thus, modeling the input wave packet (or the response function) by an appropriate moment of the Doppler formula could simplify the systems analysis, since the Fourier transforms of all moments of Doppler formulae are simple sinusoids.

Existing and future applications

Modulating frequencies in accordance with golden ratio symmetries have been used in music and electronic music systems for the last 40 years. Composer, scientist, and inventor John Chowning was a pioneer in these two applications [81]. He is best known as the developer of the Frequency Modulation (FM) synthesis algorithm [82, 83]. As a musician, in Stria and in other electronic compositions, he used the golden ratio as a strict theme that determines all aspects of the composition; further, in his music and audio systems, he utilized the Doppler formula to simulate sound received from moving sources [84-87].

Another application utilizing the golden ratio symmetry in acoustic systems is in sonar image-detection technology, which is used extensively in marine exploration, research, and investigation. A serious problem in underwater sonar radars is environmental noise, where an inappropriate filtering parameter hampers the sonar's denoising performance. An efficient method for denoising and detecting underwater sonar images based on the golden ratio has been recently proposed by, who developed an adaptive nonlocal spatial information denoising method based on the golden ratio [88]. It was shown that the proposed method was successful in removing underwater sonar image noise more effectively than other methods.

Future applications, based on the beautiful properties of the Doppler formula, might be feasible in various applications involving radars, sonars, and other localization and motion detection technologies. A rapidly developing technology is the use of the Doppler shift in Wi-Fi and smartphones for sensing human motion [89-91]. In principle, user gestures affect signal propagation and changes the sound signal waveform, thus rendering the echo signal different from the original signal. Hand gestures also alter the frequency of the received signal in a manner depicted by the Doppler effect. This effect, in addition to Time of Flight (ToF) and other detectable wave changes, is then used for the user's localization and recognition of his or her hand gestures. It is proposed here that designing the filtering system's impulse response function in a manner that incorporates the golden ratio and its moments might be effective in enhancing a system's fidelity.

Other physical manifestations of the Doppler formula and its moments

The function $F(x) = \frac{1-x}{1+x}$ shows much similarity with the exponential function, $E(x) = (1\text{-}x)\, e^{-x}$ (see Fig. 4a). The maximum difference, $F(x) - E(x)$, is ≈ 0.030720, achieved at x ≈ 0.56210, and the mean square difference (MSD), over the support (0, 1), is equal to

$$\text{MSD} = \int_0^1 \left[\frac{1-x}{1+x} - (1-x)\, e^{-x}\right]^2 dx \approx 0.0004. \qquad (29)$$

This similarity is maintained for the two families of moments, $x^n F(x)$, and $x^n F(x)$, as shown in Fig. 4b for the first two moments (n = 1, 2). Wide application of the family of exponential functions for modeling processes in many fields of science and technology gives promise that similar applications might be undertaken using the family $x^n F(x)$. Moreover, the beauty of $F(x)$ and its moments described in Section 3 (see also Table 1 and Figures 4a and 4b) justify preferring the Doppler-type formulae over the exponential ones.

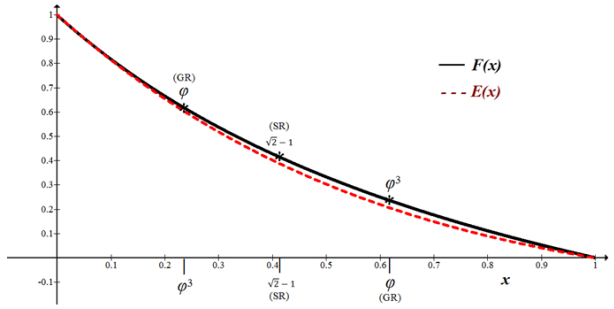

Figure 4a) *Functions F(x) and E(x) in the range (0, 1)*

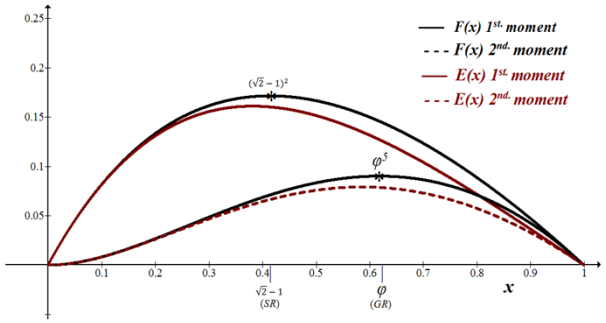

Figure 4b) *First and second moments of F(x) and E(x) in the range (0, 1)*

Notably, the first and second moments of $F(x)$, $F_1(x) = x\frac{1-x}{1+x}$, and $F_2(x) = x^2\frac{1-x}{1+x}$ emerge in other fields of physics. In Information

Relativity Theory (IRT) [92-94], for example, for a uniform body receding from the observer with constant rectilinear velocity v, IRT predicts that the observed length of a receding uniform rod of length l_0, aligned in the direction of motion equals

$$l = l_0, \frac{1-\beta}{1+\beta}, \quad \beta<1 \tag{30}$$

where $\beta = \frac{v}{V_c}$, where v is the recession velocity relative to the observer, and V_c is the velocity of the information carrier, emitted from the receding body to the observer (measured relative to its source). The observed matter density of the rod, relative to its rest-frame density ρ_0, is given by

$$\frac{\rho_m}{\rho_0} = \frac{1-\beta}{1+\beta}, \tag{31}$$

which is identical to the Doppler Formula. The relativistic momentum and energy densities in the theory are given, respectively, by the two moments $F_1(\beta)$ and $F_2(\beta)$, with maxima points equaling, respectively, the silver ratio ($\boldsymbol{\delta_s} = \sqrt{2} - 1 \approx 0.414213...$) and the golden ratio ($\varphi = \frac{\sqrt{5}-1}{2} \approx 0.618033...$) and corresponding maximal values of $\boldsymbol{\delta_s}^2 \approx 0.171573$ and $\varphi^5 \approx 0.090170$, respectively. Interestingly, the function $F_2(x) = x^2 \frac{1-x}{1+x}$ also appears in quantum mechanics [49, 53, 95, 96]. In Hardy's model of entanglement, the probability distribution function, with p_τ e n tanglement va riable, running from not entangled states to completely entangled ones, is given by

$$P(p_\tau) = p_\tau{}^2 \frac{1-p_\tau}{1+p_\tau}. \tag{32}$$

Maximized at $p_\tau = \varphi \approx 0.618033...$, with corresponding maximum equaling $\varphi^5 \approx 0.09016994....$

CONCLUDING REMARKS

Friedrich von Schiller, the German poet, playwright, writer, historian, and philosopher, defined "grace" (*Anmut*) as "beauty in motion". The theoretical investigation of the Doppler shift, as depicted in the Doppler formula, lends strong support to Schiller's definition. The "graceful" golden and silver ratios, embedded in the formula, prescribes that, irrespective of the beauty of an object's wave source, the frequency modulation of waves emitted from a moving object has beauty in itself. Our analysis revealed that the silver and golden ratios, two extremely irrational numbers, with enormous appearances in aesthetics, mathematics, and the sciences, emerge more than once in the Doppler formula and its moments. Strikingly, the silver ratio is invariant under the Doppler frequency shift transformation, such that $F(\boldsymbol{\delta_s}) = \boldsymbol{\delta_s} = \sqrt{2} - 1$ [Eq. (22)]. The golden ratio also exhibits a special symmetry in $F(\beta)$ as well [see Eqs. (23), (24)]. Further, more silver and golden ratio symmetries appear in the first three moments of the Doppler formula (see Table 1 and Fig. 4b).

Paul Dirac posited, "As time goes on, it becomes increasingly evident that the rules that the mathematician finds interesting are the same as those that nature has chosen". We cannot think of better support for Dirac's opinion than the results of the investigation undertaken here. After all, the simple and beautiful Doppler formula was dictated to Christian Doppler by nature itself. In the same line of reasoning, the fact that the base formula and its first and second moment ($F_n(x) = x^n \frac{1-x}{1+x}$, n = 0, 1, 2) emerge in more than one field of physics suggests the existence of a deeper level of reality, in which the same equation appears in various fields, are connected has yet to be discovered.

In his keynote address at the ICMC | SMC (2014) conference, John Chowning reflected about how he came to use the Golden Ratio in his music and inventions. He said, "The golden ratio fell into my 'ear lap' simply because it was 'in the air'". The results of this study confirms Chowning's intuition literally.

REFERENCES

1. Dirac PAM. Proc. R. Soc. A. Envisioning Dance on Film. 1939;59:122
2. Atiyah M. Hermann W. Biographical memoirs. Natl. Acad. Sci. 2002; 82: 1–17
3. Spadoni C. Bertrand Russell on aesthetics. Russell.1984; 4: 49–82
4. Atiyah M. Mathematics: art and science. Bull. Amer. Math. Soc. 43, 87–88
5. Zeki S, Romaya JP, Benincasa DM, et al. The experience of mathematical beauty and its neural correlates. Frontiers of Human Neuroscience. 2014; 8: 68
6. Diessner R. The Brain on Beauty: Neuroaesthetics. In: Understanding the Beauty Appreciation Trait. Palgrave Macmillan, Cham. 2019
7. Dirac PAM. Pretty mathematics. Int J Theor Phys. 1982; 21: 603–605
8. Zelinger. The quantum centennial. Nature. 2000; 408 (6813): 639
9. Kaiser P. Frequently Pondered Questions. In J. Mitoma, E. 2002; 108–112
10. Woodcock R. Capture, hold, release: an ontology of motion capture. Studies in Australasian Cinema. 2016; 10 (1): 20-34
11. Phatak MV, Patwardhan MS, Arya MS. Deep learning for motion-based video aesthetics. IEEE Bombay Section Signature Conference (IBSSC). 2019;1-6
12. Zwikker R. The beauty of motion: Exploration & reflection, kinetic art in the eye of a technical beholder. Mikroniek. 2019;1: 1-17
13. Belik J. Creation through a machine: kinetic art. Leonardo. 1988; 21: 243-246
14. Zeki S, Lamb M. The neurology of kinetic art (Review article), Brain. 1994; 117: 607-636
15. Rota GC. The phenomenology of mathematical beauty. Synthese. 1997; 111(2): 171–182

16. Engler G. Quantum field theories and aesthetic disparity, International Studies in the Philosophy of Science. 2001; 15 (1): 51-63

17. Bussey PJ. Beauty and physics. Contem Phys. 2009; 50 (3): 479-482

18. Cellucci C. Mathematical beauty, understanding, and discovery. Found Sci. 2015; 20; 339-355

19. Ivanova M. Aesthetic values in science. Philosophy Compass. 2017; 12:12433

20. Zeki S, Chén OY, Romaya JP. The biological basis of mathematical beauty. Front Hum Neurosci. 2018

21. O'Connor JJ, Robertson EF. Christian Andreas Doppler. MacTutor History of Mathematics archive. University of St. Andrews. 1998

22. Maulik D. Doppler Ultrasound in Obstetrics and Gynecology. Springer-Verlag. 2005

23. Dingle H. The Doppler Effect and the Foundations of Physics (I). The British Journal for the Philosophy of Science. 1960; 11 (41): 11-31

24. Bunn EF, Hogg DW. The kinematic origin of the cosmological redshift. Amer J Physi. 2009; 77: 688

25. Gray R, Dunning-Davies J. A review of redshift and its interpretation in cosmology and astrophysics. 2008

26. Macri LM. The 2MASS Redshift Survey in the Zone of Avoidance. Astrophys J Suppl. 2019; 245 :6

27. Mirocha J, Mirocha J. What does the first highly redshifted 21-cm detection tell us about early galaxies? Monthly Notices of the Royal Astronomical Society. 2019; 483 (2): 1980–1992

28. Cooke R. The ACCELERATION programme: I. Cosmology with the redshift drift Monthly Notices of the Royal Astronomical Society. 2020; 492(2): 2044–2057

29. Satomura S. Ultrasonic Doppler method for the inspection of cardiac function. J Acoust Soc Am. 1957; 29: 1181-1185

30. Davies MJ, Newton JD. Non-invasive imaging in cardiology for the generalist. BritHosp Medi. 2017; 78 (7): 392–398

31. Evans DH, McDicken WN. Doppler Ultrasound (2nd ed., New York: John Wiley and Sons). 2002

32. Watson-Watt R. Radar in war and in peace. Nature. 1945;156:319–324

33. Ziółkowski C, Kelner JM. Doppler-based navigation for mobile protection system of strategic maritime facilities in GNSS jamming and spoofing conditions. IET Radar, Sonar & Navigation. 2020;14(4):643–651

34. Ainslie MA. Principles of Sonar Performance Modeling. Springer. 2010

35. Leif B. Applied Underwater Acoustics. Elsevier. 2017

36. Kostaschuk R. Measuring flow velocity and sediment transport with an acoustic Doppler current profiler. Geomorphology. 2005;68(1-2):25-37

37. De Thieulloy MJ. On the use of a single-beam acoustic current profiler for multi-point velocity measurement in a wave and current basin. Sensors. 2020;20(14):3881

38. Wall HS. Analytic Theory of Continued Fractions. New York, Chelsea. 1948

39. Weisstein EW. Silver Ratio. From MathWorld--A Wolfram Web Resource. 2002.

40. Posamentier AS, Lehmann I. The glorious golden ratio Prometheus Books. 2012

41. Olsen S. The Golden Section. New York. 2006

42. De Spinadel VW. The metallic means family and multifractal spectra. Nonlinear Analysis. 1999;36:721–745

43. Gil JB, Worley A. Generalized metallic means. arXiv. 2019

44. Pittard N, Ewing M, Jevons C. Aesthetic theory and logo design: examining consumer response to proportion across cultures. Inte Mar Revi. 2007;24(4):457-473

45. Kazlacheva ZI. An investigation of the application of the golden ratio and Fibonacci sequence in fashion design and pattern making. IOP Conf. Series: Mat Sci and Engi. 2017;254:172013.

46. Shannon AG, Klamka I, van Gendc R. Generalized Fibonacci Numbers And Music. J Adva in Mathe. 2018;14(1):7564-7579

47. Ong DC. Quasiperiodic music. J Math Arts. 2020

48. Chowning J. Fifty years of computer music: Ideas of the past speak to the future. Inte Sympo Comp Mus Mod Ret. 2007;1-10

49. Hardy L. Nonlocality for two particles without inequalities for almost all entangled states. Phys Rev Lett. 1993;71:1665

50. Coldea R. Quantum criticality in an Ising chain: Experimental evidence for emergent E8 symmetry. Science. 2010;327(5962):177–180

51. Seshadreesan KP, Ghosh S. Constancy of maximal nonlocal probability in Hardy's nonlocality test for bipartite quantum systems. J Phy A: Math Theo. 2011;44(31)1-30.

52. Sun F, Ye J, Liu W. Golden ratio and quantum mechanics: Rotated Heisenberg model in a Zeeman field. ArXiv. 2015.

53. Otto H. Phase Transitions Governed by the Fifth Power of the Golden Mean and Beyond. World J Cond Mat Phys. 2020;10:135-158.

54. Petcov ST. Discrete flavour symmetries, neutrino mixing and leptonic CP violation. Eur Phys J C. 2018;78:709

55. Lindner JF, Kohar V, Kia B. Strange Nonchaotic Stars. Phys Rev Lett. 2015;114:054101

56. Mackay AL. Crystallography and the Penrose pattern. Phys A. 1982;114:609–613

57. Watson MC, Curtis JE. Rapid and accurate calculation of small-angle scattering profiles using the golden ratio. J Appl Cryst. 2013;46:1171-1177

58. Douady S, Couder Y. Phyllotaxis as a physical self-organizing growth process. Physi Revi Let. 1992;68(13):2098-2101

59. Mitchison GJ. Phyllotaxis and the Fibonacci Series. Science. 1977;196(4287):270-275

60. Klar AJS. Fibonacci's flowers. Nature. 2002;417:595

61. Zeng L, Wang G. Modeling golden section in plants. Nat Sci. 2009;19:255-260

62. Naylor M. Golden, $\sqrt{2}$, and π flowers: A spiral story. Math Magaz. 2002;75(3):163-172

63. Conte E, Khrennikov A, Federici A, et al. Variability of brain waves: A new method based on a fractal variance function and Random Matrix Theory. Chaos, Solitons & Fractals. 2009;41(5):2790-2800

64. Weiss H, Weiss V. The golden mean as the clock cycle of brain waves. Chaos, Solitons, & Fractals. 2003;18(4):643-652 [

65. Kopell NJ, Whittington MA. Temporal interactions between cortical rhythms. Fronti Neurosci. 2008;2(2):145-154

66. Van K, Cropanzano R, Kirk JJ, et al. Expanding the horizons of social justice research: Three essays on justice theory. Soc Just Res. 2015;28:229-246

67. Schuster S. A new solution concept for Ultimatum Game leading to the Golden Ratio. Scient Rep. 2017. [Google Scholar] [Crossref]

68. Suleiman R. Economic harmony: An epistemic theory of economic interactions. Games. 2017;8(1):2. [Google Scholar] [Crossref]

69. Suleiman R. On gamesmen and fair men: Explaining fairness in non-cooperative bargaining games. Royal Soc Open Sci. 2018;5:171709.

70. Iosa M. Gait phase proportions in different locomotion tasks: The pivotal role of the golden ratio. Neuro Let. 2019;699(23):127-133

71. Lorenz WE, Andres J, Franck G. Fractal Aesthetics in Architecture. Appl Math Inf Sci. 2017;11(4):971-981.

72. Smith AR, Chao KJ, Niu Q, et al. Formation of atomically flat silver films on GaAs with a silver mean quasi periodicity. Science. 1996;273(5272):226-228

73. Zhang ZD. Mathematical structure of the three-dimensional (3D) Ising model. Chin Phys B. 2013;22:030513-1–030513-15

74. Slater PB. Numerical and exact analyses of Bures and Hilbert–Schmidt separability and PPT probabilities. Quantum Inf Process. 2019;18:312.

75. Fuchs JN, Mosseri R, Vidal J. Landau levels in quasicrystals. Phys Rev B. 2018;98:165427

76. Nakakura J. Metallic-mean quasicrystals as aperiodic approximants of periodic crystals. Nat Commun. 2019;10:4235

77. Penrose R. The role of aesthetics in pure and applied mathematical research. Bull Inst Math Appl. 1974;10:266–271

78. Grünbaum B, Shephard GC. Tilings and Patterns. Freeman, New York; 1987

79. Ammann R. Aperiodic Tiles. Discr Comput Geom. 1992;8

80. Beenker FPM. Algebraic Theory of Non-Periodic Tilings of the Plane by Two Simple Building Blocks: a Square and a Rhomb. Technis Hogesc, Eindhoven. 1982

81. John Chowning. (accessed on 5.10.2020)

82. Chowning J. The synthesis of complex audio spectra by means of frequency modulation. J Audio Eng Soc. 1973;21(7):526-534

83. Chowning J, Bristow D. FM - Theory & Applications. Tokyo: Yamaha Music Foundation. 1988

84. Chowning J. Mathews' Diagram and Euclid's line: Fifty years ago (Keynote address). Proceedings of ICMC|SMC. 2014. 14-20

85. Meneghini M. Stria, by John Chowning: Analysis of the compositional process. Proceedings of the XIV Colloquium on Musical Informatics. 2003

86. Chowning J. The Simulation of Moving Sound Sources. J Audio Eng Soc. 1971;19:2-6

87. Chowning J. Method and apparatus for simulating location and movement of sound. JM Chowning. US Patent. 1972; 3: 665-705

88. Wang X. An Adaptive Denoising and Detection Approach for Underwater Sonar Image. Remote Sens. 2019;11:396.

89. Khalili A, Soliman AH, Asaduzzaman M et al . Wi-Fi Sensing: Applications and challenges. J Eng. 2020;3:87–97

90. Gupta S. Soundwave: using the Doppler Effect to sense gestures. Proc SIGCHI Conf Hum Factors Comput Syst. 2012; 1911–1914

91. Wang Z. Hand gesture recognition based on active ultrasonic sensing of smartphone: A Survey. IEEE Access. 2019;7:111897-111972

92. Suleiman R. Information relativity theory solves the twin paradox symmetrically. Phys Essays. 2016;29:304-308

93. Suleiman R. A model of dark matter and dark energy based on relativizing Newton's physics. World J Condens Matter Phys. 2018;8:130-155

94. Suleiman R. Relativizing Newton. Nova Science Publishers, N.Y; 2019

95. Schiller F. On grace and dignity. In: Curran JV, Fricker C, editors. Schiller's "On grace and dignity" in its cultural context. Essays and a new translation. Woodbridge, UK: Boydell and Brewer.2005; 123–170

96. Burke E. A philosophical enquiry into the origin of our ideas of the sublime and beautiful.